Digest Journal of Nanomaterials and Biostructures Vol. 13, No. 1, January - March 2018, p. 155 - 162

LOW-TEMPERATURE FORMATION OF 312 PHASE IN Ti-Si-C TERNARY COMPOUND

A. D. CRISAN, O. CRISAN*

National Institute for Materials Physics, PO Box MG-7, 077125, Magurele, Romania

We report on the formation of the Ti_3SiC_2 nanolaminate phase in the Ti-Si-C thin film system, using a UHV magnetron sputtering technique with top mounted sample holder, from elemental and compound targets. The formation of the Ti_3SiC_2 (or 312 phase) has been evidenced by detailed X-ray diffraction analysis followed by full-profile quantitative analysis of the obtained diffractograms. It has been proven that for deposition temperatures as low as 500°C, there is a significant amount of 312 phase obtained in the deposited films, in co-existence with the majority TiC phase. This amount increased to about 21% when the deposition temperature was raised to 650°C. The ternary 312 phase becomes predominant at around 60% relative abundance for slight off-stoichiometric, Si increased, content of the alloy, for temperatures as low as 650°C. The conditions for improving the relative abundance of the 312 phase within our experimental setup are pointed out and explained in terms of a nucleation and growth model of nanostructure formation from the amorphous precursor (?).

(Received September 8, 2017; Accepted January 23, 2018)

Keywords: ternary compounds, nanolaminates, X-ray diffraction analysis.

1. Introduction

As a part of the larger class of so-called $M_{n+1}AX_n$ (M: early transition metal, A: elements from group A, X: C or N) phase materials, Ti-Si-C ternary carbides have potential to become good candidates for a large range of applications, since they exhibit both metallic properties (good electric and thermal conductivity, thermal shock resistance) and ceramic features (high resistance to oxidation, high decomposition temperature). Recent comprehensive reviews on Ti-Si-C [1] have shown that there is still way to go in obtaining single phase nanolaminate Ti_3SiC_2 at industrially interesting temperatures (i.e. below 900°C). Phase diagrams of Ti-Si-C system show that among the possible ternary phases that might form, the Ti_3SiC_2 MAX phase is the most stable one, however, its formation is hindered by more stable binary phases. Higher-order MAX phase, i.e. Ti_4SiC_3 has been also reported to occur, whilst lower-order MAX phase, the Ti_2SiC has not been reported until now. One of the reasons for this lies in the position in the phase diagram for the 211 MAX phase, thermodynamically competing with more stable phases such as TiC, Ti_3SiC_2 and $TiSi_2$. Several techniques have been – to a varied degree of success – employed for the synthesis of the Ti_3SiC_2 phase. Ranging from bulk techniques such as the self-propagating high-temperature synthesis (SHS) [2], reactive sintering [3] and mechanical alloying [4] to thin films and coatings fabrication techniques such as chemical vapour deposition CVD [5,6] magnetron sputtering [7-9] and pulsed laser deposition PLD [10]. In spite of numerous efforts from the research community, there is little evidence of formation of compounds, either as bulk or as thin films, as a single MAX phase in the Ti-Si-C system, both as thin films or as bulk. Magnusson et al. [11] and Palmquist et al. [12] reported synthesis of epitaxial Ti_3SiC_2 (0001) single-phase film with TiC (111) seed layer magnetron sputtered at 900°C from Ti_3SiC_2 composite target. Nevertheless, as XRD patterns show a mixture of TiC and Ti_3SiC_2, the only evidence for the film being a single phase is represented by some local TEM images of ordered regions with hexagonal layered structure of Ti_3SiC_2. However,

*Corresponding author: ocrisan@yahoo.com

for a large number of applications, the single phase condition for the Ti-Si-C is not really crucial, as the presence of TiC for example does not alter significantly the co-existence of ceramic and metallic properties. It is nevertheless reported in many other papers, for example in [8] that below 900°C the only stable phase formed in such thin films is the cubic TiC structure. We have employed dc magnetron sputtering from 3 elemental targets, Ti, Si and C to deposit crystalline Ti-Si-C thin films onto Si(100). We show, by full-profile XRD analysis, successfully employed for other nanostructured multiphase materials [13-19], that crystalline structure composed of both hexagonal Ti_3SiC_2 and cubic TiC is formed for substrate temperature of as low as 550°C. The hexagonal Ti_3SiC_2 becomes the predominant phase for temperatures around 700°C for samples with little modifications of the stoichiometry (slight Si excess).

2. Experimental

The synthesis facility is a magnetron sputtering UHV facility with 3 targets radially mounted and sample holder mounted on top, facing down. The substrate is alternatively exposed to the plasma arising from elemental targets magnetron in the order Ti, Si, C. The sequential deposition may have an influence on the formation of the layered structure typical for the MAX phase Ti_3SiC_2. An initial vacuum as low as 5×10^{-8} is achieved in the deposition chamber. During the deposition the 3 magnetrons are operated in the balanced mode and the current applied is fully controlled. Magnetron powers are set such as to provide the desired stoichiometry of the 3 elements. We have established an initial set of parameters (in terms of electrical power) for the magnetrons that correspond to the desired 3:1:2 stoichiometry. These values for the 3 elemental targets are: Si: 53W, Ti: 80W, C: 160W. The deposition of thin films has been done on Si (100) commercial wafers, with no pre-deposited seed layer, at various temperatures, starting from RT up to 700C. The Ar pressure inside the chamber was set at around 6×10^{-3} mbar. The as-obtained thin films were structurally characterized using X-ray diffraction (XRD). A Bruker Advance D8 diffractometer has been used for the XRD studies. The XRD analysis is performed using the Cu Kα radiation in grazing incidence mode, typical for thin films, with an angle of incidence of the X-ray beam of 1.5º in 2Θ geometry.

3. Results

3.1. Crystallization process. Formation of crystalline 312 phase.

In order to show the evolution of crystallization in the films structure we have synthesized these films at various substrate temperatures. All depositions were done with magnetron powers corresponding to the stoichiometry of the 312 phase. The resulting samples have been measured using XRD and their corresponding patterns are depicted in Fig. 1.

The sample deposited at RT show a typical XRD pattern consisting of very broad lines centred at around 36, 40.5, 60 and 72° which correspond to the position of reflection lines of TiC (111), (200), (220) and (311) respectively. These broad lines witness the occurrence of small nanocrystalline grains having the symmetry of cubic TiC. With increasing the deposition temperature at 300°C, the XRD pattern exhibit rather similar pattern, with a slight narrowing of the main TiC lines (111) and (200) having as consequence the separation of the shoulder observed for deposition at RT, into a clear diffraction line TiC (111) for deposition at 300°C. The narrowing of the lines continues furthermore for the deposition at 500°C and the fifth TiC peak, the (222) reflection starts to appear. Situation is changed for the deposition at 550°C. Here, apart from the well-defined TiC, clear peaks belonging to the 312 hexagonal phase structure appears. The 312 (101) and 312 (103) lines are visible as satellites on each side of the TiC (111) peak while the 312 (105) line is observable as a shoulder of the TiC (200) peak. Other peaks belonging to the 312 structure are also observable for the samples deposited at and above 550°C, namely the (108) and (115) lines of the hexagonal 312 structure. The almost same phase structure, i.e. mixture of cubic

TiC and hexagonal Ti_3SiC_2, is preserved for the deposition at 650C while the narrowing of the peaks, which indicates higher degree of crystallinity and larger grains, continues.

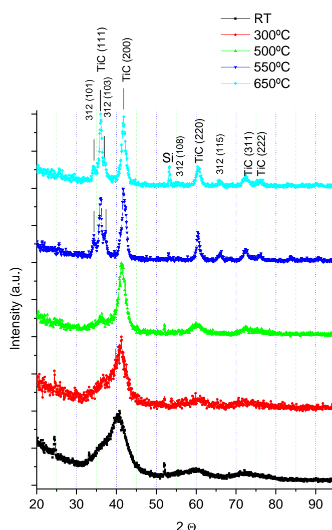

Fig. 1. XRD spectra of TiSiC films deposited at various substrate temperatures.

These observations have been made quantitative by full profile refinement of the patterns using a Rietveld-type fitting software named MAUD (Materials Analysis Using Diffraction) [25,26]. The refinement procedure implies the fit of the observed Bragg peaks from a pattern to a pseudo-Voigt line profile. Such profile accounts for the physical broadening of XRD peaks by two mechanisms. The first one is strain-related and would produce a Gaussian profile, and the other is size-related and would produce a Lorentzian profile. The pseudo-Voigt profile is thus a convolution of Lorentz and Gauss profiles. The quantitative estimation of the Lorentz relative proportion in the pseudo-Voigt profile is given by the mixing parameter which results from the fit. Based on the results of the fitting, namely peak positions, relative amplitude, full width at half maximum (FWHM) and the mixing parameter, we can calculate the lattice parameters of the observed phases. The calculation takes into account all observed peaks, belonging to the same phase, TiC and Ti_3SiC_2, being more reliable than calculations based on only few observed lines. The fit provides also the relative abundance of the observed phases that give rise to peaks in the XRD pattern. For the calculation of the average grain size, which is defined here as the average size of the crystallographically coherent domain, it is largely practiced the use of Scherrer's formula which links the FWHM to the average grain size in an inverse proportionality relationship. It is known nevertheless, that the method does not take into account the specific profile of the diffraction line or its possible asymmetry. A more precise approach is represented by the integral breadth method [26-28].

This method calculates, using the lattice parameters, FWHM and mixing parameters of each Bragg reflection, the average crystallographically coherent domain size associated with the average size of the grains and the root mean square lattice microstrain. Here, the lattice microstrain is defined as the amount (change in size or volume) by which a crystal lattice deforms under stress or force and it is given as a ratio of the deformation to the initial lattice size, being a non-dimensional parameter.

Table 1: The lattice parameters for the phases indexed in XRD patterns of Fig. 2, their relative abundance and the average grain size as obtained from the full profile refinement of the XRD patterns and calculations using the integral breadth method.

Dep. Temp.	Phases observed						
	TiC			Ti_3SiC_2			Amorph.
	Lattice params	Mean grain size	Relative fraction (%)	Lattice params	Mean grain size	Relative fraction (%)	Relative fraction (%)
RT -	a=4.36±0.02	6.8	64	-	-	-	36
300C	a=4.35±0.03	8.4	71	-	-	-	29
500C	a=4.345±0.007	16.4	77	a=2.99±0.03 c=17.88±0.2	11.2	8	15
550C	a=4.337±0.005	24.3	72	a=3.021±0.015 c=17.81±0.09	18.6	18	10
650C	a=4.321±0.003	28.7	69	a=3.054±0.008 c=17.78±0.07	21.1	23	8

The results of the fitting of the XRD patterns from Fig. 2 are given in Table 1.

It can be observed that the calculated average grain size follows the visual observations about the narrowing of the XRD lines. With increasing the deposition temperature the average grain size of the TiC phase increases from an estimated value of about 7 nm up to about 30 nm for the sample deposited at 650°C. It has to be mentioned that in the case of samples deposited at low temperatures (RT, 300°C) the XRD lines being very broad, both positions and linewidths of the lines are determined with a high degree of uncertainty, therefore the derived parameters, such as lattice parameters and especially the average grain size must be cautiously considered, being merely a crude estimation of these values. The situation is different in the case of samples annealed at higher temperatures where the peaks are well resolved and the errors are substantially smaller. There is also an important amorphous fraction in the samples, more important in the samples deposited at low temperatures, which was expected. This fraction which represents mainly the intergranular regions between the well-formed TiC and Ti_3SiC_2 grains becomes much smaller for samples deposited at higher temperatures, as a consequence of increased crystallinity and larger grain sizes. The decrease of the relative abundance of the amorphous phase at the expenses of formation of Ti_3SiC_2 phase is to be explained by the means of the nucleation and growth model, applicable in intermetallic alloys [29]. The Ti_3SiC_2 phase starts to form alongside TiC for deposition temperatures as low as 500°C (8% relative fraction of observed Ti_3SiC_2 phase) while the coating deposited at 550°C shows clear and well resolved Ti_3SiC_2 peaks, its relative fraction amounting to 18%. It reaches a maximum of 23% at 650°C deposition temperature, in the same stoichiometry conditions. The lattice parameter of TiC cubic phase follows a decreasing trend with increasing the deposition temperature as a result of increase of the ordering, approaching to the theoretical bulk value for TiC, in the case of the sample deposited at 650°C. It is interesting to note that the lattice parameters of Ti_3SiC_2 evolve differently with the deposition temperature. While the *a* parameter increases with increasing temperature, with about 2% from 500°C to 650°C deposition temperature, the *c* parameter decreases with about 0.5% for the same range of deposition temperatures. This suggests an enhanced ordering rate in the basal plane defined by the (*ab*) plane of the hexagonal unit cell rather than along *c* axis. Nevertheless these results are to be considered only as a trend since the errors in the lattice parameters calculation are quite high especially at lower deposition temperatures.

The formation of the 312 phase in the Ti-Si-C system for deposition temperatures as low as 500-550°C represents a significant breakthrough, as it has been reported in a variety of previous papers that the 312 phase does not form as single phase in thin films and coatings until 900°C [7-

9]. The only phase reportedly stable below 900°C, for the stoichiometry we have used, has been found to be the cubic TiC.

3.2. Enhancement of 312 relative proportion. Influence of Si content.

We have observed that for temperatures as low as 500-550°C, a significant amount of Ti_3SiC_2 phase is formed, together with the cubic TiC. Nevertheless, as the deposition temperatures are quite low, a significant amorphous residual fraction still exists in the samples and the crystallinity, defined here as the average grain size of the crystal phases, is still low. We have searched for a way to maximise the relative amount of Ti_3SiC_2 phase and minimise the amount of TiC, in the way of achieving single 312 phase in the films. The challenge is twofold. On one hand, in order for this deposition technique to be economically viable, the deposition temperatures must be kept as low as possible, below the 900°C threshold where most of the Ti_3SiC_2 phases reported until now were formed, while still maintaining a high degree of crystallinity of the samples. On the other hand, a slight imbalance in the stoichiometry might be sought in order to impeach the formation of TiC in favour of Ti_3SiC_2 phase. Our idea was to slightly increase the Si content in order to reduce the TiC amount by facilitating enough Si atoms that may promote furthermore formation of the hexagonal ternary phase. The enhancement of Si content must be considered though with precautions as a too high Si content may lead to formation of other stable phase in that region of the phase diagram, i.e. the undesired $TiSi_2$ orthorhombic phase.

With this in mind, we have synthesized a series of thin films deposited in same conditions (Ar pressure 6 x 10^{-3} mbar, 150 min deposition time, 700°C deposition temperature) but with increasing Si content, measured by the increasing the power on the Si magnetron, from 45W to 85 W while keeping the power on the other two magnetrons, the Ti and the C, constant: 160W for the Ti and 260W for the C. The resulting samples have been structurally characterized using X-ray diffraction in grazing-incidence 2θ geometry, with an incidence angle ω = 1.5 degrees (the angle of incidence of the X-ray beam to the film surface plane). The obtained XRD patterns are depicted in Fig. 2

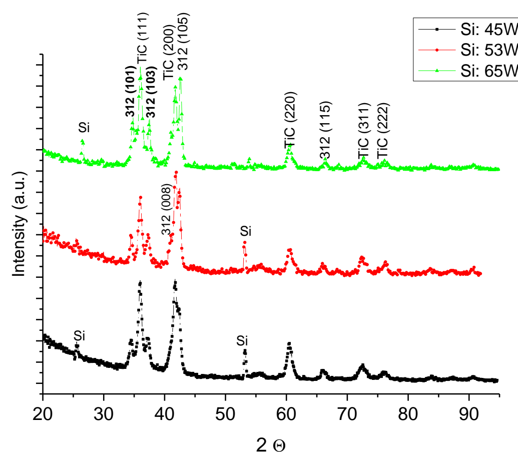

Fig. 2. XRD spectra of the series of samples synthesized with a variable Si content

It can be observed that the XRD peaks are well defined in all cases suggesting an improvement of the overall crystallinity. The formation of satellite peaks on each side of the main TiC peaks, the peaks signaling the occurrence of the Ti_3SiC_2 phase are obviously formed. The relative intensity of those satellite peaks, namely the (101), (103), (008) and (105) of the Ti_3SiC_2 phase increases upon increasing the Si magnetron power. Apart from TiC and Ti_3SiC_2 phases and a small residual amorphous phase, no other phase has been identified in the patterns. The Si excess in the range covered by the magnetron power we have used was not high enough to produce occurrence of TiSi binary phases.

For clarity we present in the Fig. 3 the comparison in the range of interest (30-50 degrees) of the XRD patterns of samples with extreme Si powers: the one deposited with 45W and the other one deposited with 85W power of the Si magnetron.

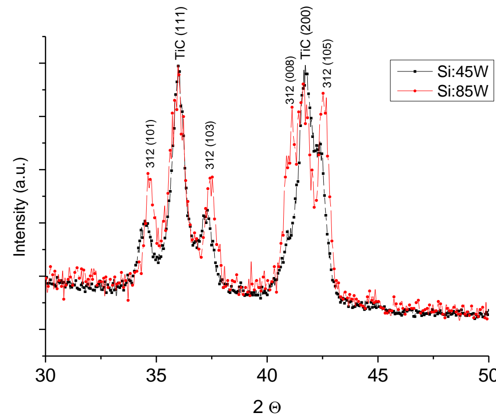

Fig. 3. Central part of the X-ray diffractograms of the samples deposited with Si target power of 45W and 85W respectively

It can be seen that while the TiC peaks (111) and (200) are at almost the same intensity for the two different patterns, all the 312 main peaks show strong increase in intensity, even a 3-fold increase for the (008) peak, for the 85W Si sample than for the 45W Si sample. These observations have been made quantitative by numerical fitting and calculations following the procedures described above. In the Table 2, the results of the fitting of XRD patterns: lattice parameters, average grain size, relative fraction of the phases observed, are presented as a function of the Si content translated into Si magnetron power during deposition.

Table 2: The lattice parameters for the phases indexed in XRD patterns of Figs. 3 and4, their relative abundance and the average grain size as obtained from the full profile refinement of the XRD patterns and calculations using the integral breadth method.

Sample / Si content	Phases observed						
	TiC			Ti_3SiC_2			Amorph.
	Lattice param	Mean grain size	Relative fraction (%)	Lattice params	Mean grain size	Relative fraction (%)	Relative fraction (%)
Si: 45W	a=4.325±0.002	21.2	53	a=3.069±0.007 c=17.61±0.07	20.1	41	6
Si: 53W	a=4.324±0.003	22.7	44	a=3.068±0.01 c=17.65±0.07	25.8	48	8
Si: 65W	a=4.321±0.007	22.2	39	a=3.085±0.01 c=17.57±0.07	30	55	6
Si: 85W	a=4.325±0.006	20	35	a=3.064±0.016 c=17.61±0.013	25.3	60	5

The main effect of the increasing Si content in the microstructure of the as-deposited thin films is, as it can be seen from the table 2, is the steady and continuous increase of the relative fraction of Ti_3SiC_2 from 40% to about 60% for the maximum Si magnetron power applied of 85W. We have proven thus, that it is possible to provide Ti-Si-C magnetron sputtered thin films with

majority 312 MAX phase at temperatures well below the 900°C threshold reported until now, by slight off-stoichiometry deviations in the Si content. If this off-stoichiometry is finely tuned and perhaps accompanied by slight increase of the deposition temperature up to 750°C, we can eventually achieve a single phase Ti_3SiC_2 when magnetron sputtering from elemental targets, without the need of oriented seed layer.

4. Conclusions

In the framework of the intensified research efforts for achieving the 312 ternary phase of the Ti-Si-C system, we have made use of a magnetron sputtering facility to depose compound ternary thin film alloys with alternating elemental deposition from Ti, Si and C sputtering targets. By using full-profile Rietveld-type analysis of the X-ray diffractograms on the obtained samples, we have been able to quantitatively assess the phase composition in the alloy. We have accurately obtained the relative fraction of the obtained phases, i.e. the binary TiC and the ternary Ti_3SiC_2 and we have proven that by finely tuning the magnetron power of the Si sputtering target, we obtain an alloy where the ternary phase of interest Ti_3SiC_2 becomes predominant for deposition temperatures as low as 650°C. This finding open good perspectives on the way of obtaining single phase Ti_3SiC_2 in these systems.

Acknowledgements

Financial support from Romanian Ministry of Research and Innovation via project PN-III-P4-ID-PCE-2016-0833 is gratefully acknowledged.

References

[1] H.B. Zhang, Y.W. Bao, Zhou, Y.C, J. Mater. Sci. Technol. **25**, 1 (2009).
[2] J. Lis and R. Pampuch: Solid State Ionics **101**, 59 (1997).
[3] C. Racault, F. Langlais and R. Naslain: J. Mater. Sci. **29**, 3384 (1994).
[4] D.P. Riley, E.H. Kisi and D. Phelan: J. Euro. Ceram. Soc. **26**, 1051 (2006).
[5] E. Pickering, W.J. Lackey, S. Crain, Chem. Vap. Deposition **6**, 289 (2000).
[6] S. Jacques, H. Di-Murro, M.P. Berthet and H. Vincent: Thin Solid Films **478**, 13 (2005).
[7] J. Emmerlich, H. Hogberg, S. Sasvari, P.O.A. Persson, L. Hultman, J.P. Palmquist, U. Jansson, J.M. Molina-Aldareguia and Z. Czigany: J. Appl. Phys. **96**, 4817 (2004).
[8] J.P. Palmquist, S. Li, P.O.A. Persson, J. Emmerlich, O. Wilhelmsson, H. Hogberg, M. I. Katsnelson, B. Johansson, R.Ahuja, O.Eriksson, L.Hultman and U. Jansson: Phys. Rev. B **70**, 165401 (2004).
[9] H. Hogberg, L. Hultman, J.Emmerlich, T. Joelsson, P. Eklund, J.M. Molina-Aldareguia, J.P. Palmquist, O. Wilhelmsson and U. Jansson: Surf. Coat. Tech. **193**, 6 (2005).
[10] J.J. Hu, J.E. Bultman, S. Patton and J.S. Zabinski, Tribology Lett. **16**, 113 (2004).
[11] M. Magnusson, J. -P. Palmquist, , M. Mattesini, S. Li, R. Ahuja, O. Eriksson, J. Emmerlich, O. Wilhelmsson, P. Eklund, H. Högberg, L. Hultman, U. Jansson, Phys. Rev. B **72**, 245101 (2005).
[12] J.-P. Palmquist and U. Jansson, Appl. Phys. Lett. **81**, 835 (2002).
[13] O. Crisan, A.D. Crisan, J. Alloys. Compd. **509**(23), 6522(2011).
[14] O. Crisan, A.D. Crisan, N. Randrianantoandro, et al. J. Alloys. Compd. **440**(1-2), L3 (2007).
[15] M. Rosenberg, V. Kuncser, O. Crisan, et al. J. Magn. Magn. Mater. **177**, 135 (1998).
[16] V.R. Reddy, O. Crisan, A. Gupta, et al. Thin Solid Films **520**(6), 2184 (2012).
[17] A.D. Crisan, O. Crisan, J. Phys. D: Appl. Phys. **44**(36), 365002 (2011).
[18] A.D. Crisan, J. Optoelectron. Adv. M. **12**(2), 250 (2010).

[19] A.D. Crisan, O. Crisan, Mater. Sci. Technol. **28**(4), 460 (2012).
[20] O. Crisan, K. von Haeften, A.M. Ellis, C. Binns, J. Nanopart. Res. **10** (suppl.1), 193-198 (2008).
[21] O. Crisan, J.M. Greneche, J.M. Le Breton, A.D. Crisan, Y. Labaye, L. Berger, G. Filoti, Eur. Phys. J. B **34**(2), 155-162 (2003).
[22] O. Crisan, J.M. Le Breton, M. Nogues, F. Machizaud, G. Filoti, J. Phys. Condens. Mat. **14**(47), 12599-12609 (2002).
[23] O. Crisan, Y. Labaye, L. Berger, J.M.D. Coey, J.M. Greneche, J. Appl. Phys. **91**(10), 8727-8729 (2002).
[24] M. Seqqat, M. Nogues, O. Crisan, V. Kuncser, L. Cristea, A. Jianu, G. Filoti, J.L. Dormann, D. Sayah, M. Godinho, J. Magn. Magn. Mater. **157,** 225-226 (1996).
[25] D. Balzar and H. Ledbetter, J. Appl. Cryst. **26,** 97 (1993).
[26] D. Balzar, J. Res. Natl. Inst. Stand. Technol. **98**, 321 (1993)
[27] B.E. Warren, X-ray Diffraction, Addison Wesley, Reading, MA, 1969
[28] H.P. Klug and L.E. Alexander, X-ray Diffraction Procedures 2nd edition John Wiley, New York, 1974.
[29] J.M. Le Breton, A. Zorkovska, M. Kasiarova, J. Phys: Condens. Matter. **16**(30), 5555 (2004).